OPEN

Citation: Transl Psychiatry (2013) 3, e338; doi:10.1038/tp.2013.105

www.nature.com/tp

ORIGINAL ARTICLE

dcc orchestrates the development of the prefrontal cortex during adolescence and is altered in psychiatric patients

C Manitt[1,8], C Eng[1,8], M Pokinko[1], RT Ryan[1], A Torres-Berrío[1], JP Lopez[1], SV Yogendran[1], MJJ Daubaras[1], A Grant[1], ERE Schmidt[2], F Tronche[3], P Krimpenfort[4], HM Cooper[5], RJ Pasterkamp[2], B Kolb[6], G Turecki[1], TP Wong[1], EJ Nestler[7], B Giros[1,3] and C Flores[1]

Adolescence is a period of heightened susceptibility to psychiatric disorders of medial prefrontal cortex (mPFC) dysfunction and cognitive impairment. mPFC dopamine (DA) projections reach maturity only in early adulthood, when their control over cognition becomes fully functional. The mechanisms governing this protracted and unique development are unknown. Here we identify *dcc* as the first DA neuron gene to regulate mPFC connectivity during adolescence and dissect the mechanisms involved. Reduction or loss of *dcc* from DA neurons by Cre-lox recombination increased mPFC DA innervation. Underlying this was the presence of ectopic DA fibers that normally innervate non-cortical targets. Altered DA input changed the anatomy and electrophysiology of mPFC circuits, leading to enhanced cognitive flexibility. All phenotypes only emerged in adulthood. Using viral Cre, we demonstrated that *dcc* organizes mPFC wiring specifically during adolescence. Variations in DCC may determine differential predisposition to mPFC disorders in humans. Indeed, *DCC* expression is elevated in brains of antidepressant-free subjects who committed suicide.

Translational Psychiatry (2013) **3,** e338; doi:10.1038/tp.2013.105; published online 17 December 2013

Keywords: dopamine; neurodevelopmental disorders; neural circuit formation; prefrontal cortex dysfunction; resilience

The establishment of dopamine (DA) connectivity within the medial prefrontal cortex (mPFC) is a process that is ongoing until adulthood.[1–4] During adolescence, specifically, the mesocortical DA circuit undergoes an intense period of maturation during which DA fiber inputs increase in density and become more populated with presynaptic terminals. Concurrent with these developmental changes, local mPFC neurons shift towards a mature state of responsiveness to the modulatory effects of DA.[5,6] Correspondingly, higher order cognitive processes that are dependent on mPFC function also undergo profound changes during adolescence and in fact only become fully functional in adulthood.[6,7] Impairments in cognition are a core feature of a number of psychiatric diseases associated with subtle alterations in mPFC circuitry, such as schizophrenia, depression and drug abuse.[8–11] Indeed, adolescence is a period of high risk for these psychopathologies. Unraveling the mechanisms that coordinate the unique developmental course of mesocortical DA neurons and their impact on postsynaptic circuits is crucial, and yet these mechanisms are completely unknown.

Deleted in colorectal cancer (DCC), the receptor for the guidance cue netrin-1, is expressed in the brain across the lifespan.[12] Our past work suggests that DCC signaling may be a component of a molecular mechanism that is recruited during the establishment of mPFC DA synaptic connectivity during adolescence.[13,14] We have demonstrated that *dcc* haploinsufficiency leads to pre- and postsynaptic structural alterations that appear to be unique to mPFC DA circuitry. Specifically, *dcc* haploinsufficient mice show increased DA synaptic input and DA release in the mPFC and reduced dendritic spine density of layer V pyramidal neurons. These alterations emerge only in adulthood, suggesting that DCC may be required precisely during the late maturation of mesocortical DA connectivity.[13,14] Importantly, *dcc* haploinsufficiency has been identified recently in the human population.[15,16] Although a number of genes have been identified as having a role in the embryonic development of DA neurons, *dcc* may be the first candidate gene implicated in their unique adolescent development.

Here, we first sought to confirm that DCC during development is required for appropriate mPFC function in adulthood using the same model of *dcc* haploinsufficiency as in our previous studies. In these experiments, we examined adult mPFC neuronal function with electrophysiological and behavioral approaches. Next, we undertook to identify the precise temporal window of DCC-mediated effects on mPFC DA circuit development and to dissect the underlying mechanisms. To this end, we generated mice with a loss-of-function mutation of the *dcc* gene in DA neurons exclusively by applying Cre-lox and viral-mediated gene transfer technologies. Both *dcc* heterozygous and *dcc* homozygous conditional mice survive to adulthood and appear normal. Thus, we were able to explore for the first time the effects of *dcc reduction* as well as *dcc loss* on postnatal brain development. Finally, we measured *DCC* expression in postmortem brains of depressed suicide completers to begin corroborating a link between *DCC* and psychiatric disorders of mPFC dysfunction.

[1]Department of Psychiatry, Douglas Mental Health University Institute, McGill University, Montreal, QC, Canada; [2]Department of Neuroscience and Pharmacology, Rudolf Magnus Institute of Neuroscience, University Medical Center Utrecht, Utrecht, The Netherlands; [3]UMR 7224 CNRS and Université Pierre et Marie Curie, Paris, France; [4]Division of Molecular Genetics, Centre for Biomedical Genetics, Cancer Genomics Centre, The Netherlands Cancer Institute, Amsterdam, The Netherlands; [5]The University of Queensland, Queensland Brain Institute, Brisbane, QLD, Australia; [6]Canadian Centre for Behavioural Neuroscience, University of Lethbridge, 4401 University Drive, Lethbridge, AB, Canada and [7]Fishberg Department of Neuroscience and Friedman Brain Institute, Mount Sinai School of Medicine, New York, NY, USA. Correspondence: Dr C Flores, Department of Psychiatry, Douglas Mental Health University Institute, 6875 boulevard LaSalle, Montreal, QC, Canada H4H 1R3.
E-mail: cecilia.flores@mcgill.ca
[8]These authors contributed equally to this work.
Received 10 October 2013; accepted 21 October 2013

MATERIALS AND METHODS

Animals

All experiments and procedures were performed in accordance with the guidelines of the Canadian Council of Animal Care and the McGill University/Douglas Mental Health University Institute Animal Care Committee. Experiments were conducted in juvenile (postnatal day (PND) 21 ± 1) and adult (PND 75 ± 15) male mice. Adult female mice were used in the sensorimotor-gating experiments. Mice were weaned at PND 20 and housed with same-sex littermates.

dcc haploinsufficient mice. *dcc* haploinsufficient male mice were maintained on a BL/6 background and bred with wild-type BL/6 female mice.[17] These mice have targeted disruption of exon 3 and complete loss of DCC expression in the affected allele.[18]

dcc conditional mice. The loss-of-function mutation in *dcc* in DA neurons exclusively was done using the Cre-loxP recombination system. We crossed a line in which Cre-recombinase recognition sequence (loxP)-insertions flanked exon 23 of the *dcc* gene (*dcc*-floxed mice; $dcc^{lox/+}$) with a line in which iCre expression is regulated by the DA transporter (DAT; BAC-*DATiCre* mice). We generated heterozygous ($dcc^{lox/+}DAT^{cre}$), homozygous ($dcc^{lox/lox}DAT^{cre}$) and floxed control ($dcc^{lox/+}$ or $dcc^{lox/lox}$) groups. For details regarding the $dcc^{lox/+}$ and BAC-*DATiCre* mice and the characterization experiments conducted on the conditional offspring, see the Supplementary Information.

Behavioral testing

Tests for the attentional set-shifting task (ASST), the elevated plus maze, locomotor activity and prepulse inhibition of acoustic startle response were conducted as described in the Supplementary Information.

Stereological counts

The total number of DA neurons in the VTA and the total number of TH-positive varicosities in the mPFC and nucleus accumbens (NAcc) were evaluated using a stereological fractionator sampling design, with the optical fractionator probe of the Stereo Investigator software (MicroBrightField, Williston, VT, USA) as reported previously[13] and as described in detail in the Supplementary Information.

Golgi–Cox staining

The brains were processed for Golgi–Cox staining, as described.[13] Using Neurolucida (MicrobrightField), we analyzed basilar dendritic spine density of layer V pyramidal neurons in the pregenual mPFC (including Cg1, PrL and IL subregions) and dendritic spine density of medium spiny neurons in the NAcc as repored previously[13,17] and as described in detail in the Supplementary Information.

Viral-mediated deletion of *dcc*

To induce selective inactivation of the *dcc* gene in VTA neurons, we microinjected adeno-associated viruses (AAV-2;[19]) into the VTA of heterozygous and homozygous *dcc*-floxed ($dcc^{lox/lox}$) mice at either PND 21 or PND 60. Mice received bilateral VTA stereotaxic infusions of AAV expressing a CreGFP fusion protein (AAV-CreGFP) or a control GFP-expressing virus (AAV-GFP). We performed stereological counts of GFP-labeled TH-positive neurons 1 month after surgery to assess the degree of infection. For details see the Supplementary Information.

Electrophysiology

Brain slices from adult male *dcc* haploinsufficient and wild-type mice were prepared for current-clamp recordings. Electrophysiological data were analyzed off-line using Clampfit (Molecular Devices) for input resistance estimation and firing property analysis. After a recording session, the slices were fixed by immersion in 4% PFA, and the biotin-filled recorded neurons were visualized using a DAB kit (Vector Labs, Burlingame, CA, USA). For details see the Supplementary Information.

Quantification of *DCC* expression in human brain samples

DCC expression was quantified in prefrontal cortex (Brodmann area 44; BA44) tissue samples obtained from a group of suicide completers ($N = 30$) and age-matched sudden-death controls ($N = 35$), using qRT–PCR. For details regarding subject information and quantification, see the Supplementary Information.

Statistical analysis

See the Supplementary Information.

RESULTS

Altered mPFC function in *dcc* haploinsufficiency

We have previously shown that adult *dcc* haploinsufficient mice exhibit an increase in DA connectivity in the mPFC as well as structural modifications in layer V mPFC pyramidal neurons selectively.[13,17] To determine whether these pre- and postsynaptic alterations produce changes in mPFC function, we assessed the electrophysiologial properties of layer V mPFC pyramidal neurons in adult *dcc* haploinsufficient mice (Figure 1). For these experiments, we looked at the effects of *dcc* haploinsufficiency because it is a transgenic model that has a clear ethological validity; *dcc* haploinsufficiency occurs in the human population.[15,16]

Using the current-clamp technique, we injected stepwise depolarizing currents into Layer V mPFC pyramidal neurons of adult *dcc* haploinsufficient mice. More current was required to trigger a first spike in neurons from *dcc* haploinsufficient mice than wild-type controls (Figure 1a). Consistently, neurons from *dcc* haploinsufficient mice had a higher action potential threshold (Figure 1b). Even at high currents, neurons from *dcc* haploinsufficient mice tended to display fewer action potentials than their wild-type counterparts (Figure 1c). Resting membrane potentials and input resistance were not different between genotypes (data not shown). We confirmed the identity and location of the recorded cells by injecting biotin at the time of recording. These results show that layer V mPFC pyramidal neurons have reduced excitability. These findings now confirm that DCC is required for the development of local mPFC circuitry and, in turn, for the normal function of the adult mPFC.

To identify how DCC is involved in mPFC-dependent cognitive processes, we assessed cognitive flexibility in the *dcc* haploinsufficiency model. Thus, we examined the ability of adult *dcc* haploinsufficient mice to make adaptive responses to a changing environment by successfully shifting their attention between two stimulus dimensions (digging medium to odor). We used the Attentional Set-Shifting Task[20] in which mice were trained to dig for a food reward placed in one of two small pots each marked by a unique combination of a digging medium and an odor. Mice had to perform the following: (1) a simple discrimination (s.d.) between two digging mediums, (2) a compound discrimination (CD) during which an odor dimension was introduced, but digging medium remained the rewarded cue, (3) an intradimensional shift (ID) in which both digging medium and odor were changed, but digging medium remained the rewarded cue and (4) an extradimensional shift (ED) in which odor, instead of digging medium, became the rewarded stimulus dimension. Performance during the ED task, specifically, is what is considered to be a measure of cognitive flexibility and is known to be dependent on mPFC function. ED set shifting is impaired following lesion of the mPFC in rodents and of the dorsolateral PFC in primates, but performance in other aspects of the task remains intact.[20,21]

There were no differences in discrimination learning between genotypes, as they performed similarly in the SD, CD and ID tasks (Figure 1d). Remarkably, however, *dcc* haploinsufficient mice showed greater cognitive flexibility; they performed significantly better in the ED part of the task than wild-type control littermates (Figure 1d). Increased cognitive flexibility in *dcc* haploinsufficient mice did not result from differences in anxiety. Mice of both

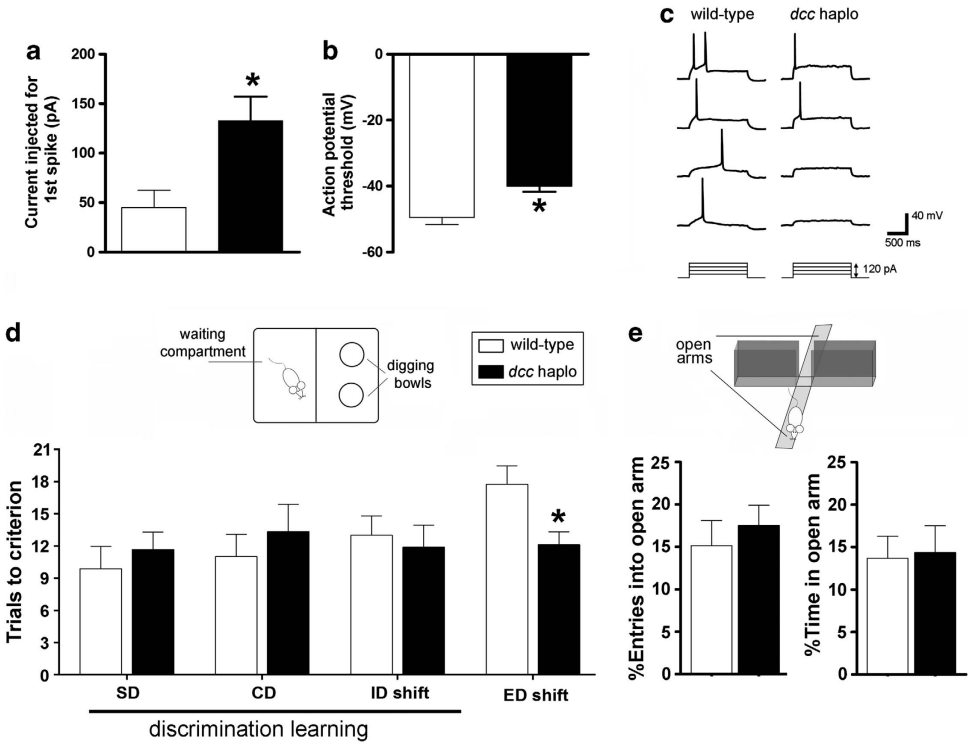

Figure 1. Improved behavioral flexibility and reduced excitability of layer V mPFC pyramidal neurons in *dcc* haploinsufficient mice. (**a**–**c**) Depolarizing current steps (30pA) were injected into layer V pyramidal neurons of the pregenual mPFC (spanning the cingulate 1 and prelimbic subregions) to estimate the rheobase current, which was defined as the first current step capable of eliciting one action potential. (**a**) The average injected current that was required to trigger an action potential (1st spike) was significantly higher in adult *dcc* haploinsufficient mice compared with wild-type littermate controls (wild-type: $n=6$; *dcc* haploinsufficient: $n=8$; $t_{(12)}=3.013$, $P=0.0108$). (**b**) The average action potential threshold of Layer V pyramidal neurons is significantly higher in *dcc* haploinsufficient mice (wild-type: $n=6$; *dcc* haploinsufficient: $n=8$; $t_{(12)}=3.788$, $P=0.0026$. (**c**) Representative membrane potential traces recorded from mPFC layer V pyramidal neurons of wild-type and *dcc* haploinsufficient mice. Note that more current steps are needed to trigger action potential formation in *dcc* haplosinsufficient mice. (**d**) *dcc* haploinsufficient mice exhibit increased behavioral flexibility in the Attentional Set-Shifting Task. No differences were observed between *dcc* haploinsufficient and wild-type mice in the mean number of trials to criterion required to solve the SD, CD, and ID tasks, indicating no differences in discrimination learning between the two genotypes (wild-type: $n=8$; *dcc* haploinsufficient: $n=9$; two-way repeated measures ANOVA, no significant main effect of genotype: $F_{(1,15)}=0.285$, $P=0.601$; no significant interaction: $F_{(2,30)}=0.463$, $P=0.634$). However, *dcc* haploinsufficient mice performed better than wild-type littermates in the ED part of the task ($t_{(15)}=2.723$, $P=0.0157$), indicating superior mPFC-dependent behavioral flexibility in these mice. (**e**) The difference in performance in the Attentional Set-Shifting Task is not attributable to genotypic differences in anxiety. There were no differences between genotypes in either the percent of entries into, or the percentage of time spent in, the open arm of the elevated plus maze, indicating that both groups displayed comparable levels of anxiety. Statistical analysis was performed on the raw data (wild-type: $n=17$; *dcc;* haploinsufficient: $n=15$; number of entries into open arm: $t_{(30)}=0.081$, $P=0.936$; time spent in open arm: $t_{(30)}=0.214$, $P=0.832$).

genotypes spent a similar amount of time in, and had a similar number of entries into, the open arm of an elevated plus maze (Figure 1e).

Notably, deficits in cognitive flexibility have been observed in DA-related psychopathologies associated with mPFC dysfunction, including schizophrenia, depression and drug abuse.[8–10] We have previously proposed that reduced DCC confers protection against developing traits associated with these psychiatric disorders and that this protection results from selective changes in mPFC function.[22] The greater cognitive flexibility observed in adult *dcc* haploinsufficient mice, which is associated with reduced excitability of layer V mPFC pyramidal neurons, extends and further supports *dcc* haploinsufficiency as a model of resilience. These findings warrant investigating whether *dcc* heterozygous humans display enhanced adaptive responses as well as resilience to certain psychopathologies.

In the next series of experiments, we aimed to dissect how DCC expression within DA neurons contributes to the development of mPFC circuitry, which in turn has a profound, yet specific, impact on mPFC function and cognition.

The pre- and postsynaptic organization of mPFC DA circuitry requires *dcc* function within DA neurons

DCC-floxed DAT-iCre mice. *dcc* haploinsufficiency leads to pre- and postsynaptic structural and functional changes in mPFC DA circuitry, including altered mPFC-dependent cognitive flexibility. Our next goal was to begin dissecting the precise mechanisms mediating these effects. Thus, we examined whether DCC signaling *within* DA neurons orchestrates their innervation to the mPFC and in turn the organization of local mPFC circuitry. We bred conditional mice in which the *dcc* gene undergoes a loss-of-function mutation in DA neurons, exclusively, using a Cre-loxP recombination system. This was accomplished by crossing *dcc*-floxed mice ($dcc^{lox/+}$;[23]) with DAT-iCre mice (DAT^{cre};[24]). *dcc*-floxed mice carry two loxP sites in the intronic sequences flanking exon 23 of the *dcc* gene. Exon 23 contains 163 nucleotides and encodes an amino-acid sequence that spans a portion of the extracellular and transmembrane domains of DCC. We confirmed by western analysis that the loxP insertions do not disrupt DCC expression and that both $dcc^{lox/+}$ and $dcc^{lox/lox}$ genotypes can serve as control groups (data not shown).

To verify Cre-mediated recombination within ventral tegmental area (VTA) DA neurons, we amplified a portion of the *dcc* gene that includes the region flanked by the loxP sites (Figure 2a, see schematic). The predicted length of the wild-type allele PCR product is of ~5700 bp, which is too large to amplify. Consistent with this, no band was obtained from control mice (Figure 2a). In contrast, the product obtained from conditional mice was of 374 bp, confirming Cre-mediated recombination. Cre-recombination was specific to DA neurons because PCR conducted with DNA extracted from the red nucleus of $dcc^{lox/lox}$DAT^{cre} mice did not yield an amplification product (data not shown). The red nucleus has robust DCC expression but lacks DA neurons. Consistent with our PCR experiment confirming Cre-mediated recombination of *dcc* and deletion of exon 23, *in situ* hybridization using a DIG-labeled riboprobe against exon 23 shows a marked decrease in the number of DA cells positive for *dcc* (data not shown). Deletion of exon 23 produces a frameshift mutation that results in a number of new putative premature stop codons. To determine whether an mRNA product is transcribed from the recombined *dcc* allele, we conducted RT–PCR on cDNA of VTA tissue taken from conditional mice. We found two bands; one corresponding to the wild-type allele (amplified from *dcc*-expressing VTA cells that do not express DAT) and one corresponding to the recombined mRNA product, which was barely detectable (Figure 2b). Together, our findings indicate that *dcc* mRNA from the recombined *dcc* allele is present at levels barely above detection and is therefore likely unstable. Consistent with these findings, two other groups reported a loss of DCC function in *dcc*-floxed mice that were crossed with lines that express Cre under a ubiquitous promoter or a promoter of the *alpha-subunit of the Calcium-dependent kinase II* gene.[23,25]

Indeed, the number of VTA DA neurons expressing DCC protein in adult conditional homozygous ($dcc^{lox/lox}DAT^{cre}$) mice was markedly reduced in comparison with *dcc*-floxed controls; this pattern was maintained across the rostro-caudal axis (Figure 2c). We next assessed the extent of the decrease in DCC expression across genotypes by conducting western analysis on tissue punches from the nucleus accumbens (NAcc). In contrast to the VTA, DA fibers are the exclusive source of DCC expression in the NAcc. We found that DCC levels are decreased by ~54% in $dcc^{lox/+}DAT^{cre}$mice and by ~77% in $dcc^{lox/lox}$DAT^{cre} mice (Figure 2d).

To determine whether the absence (that is, $dcc^{lox/lox}DAT^{cre}$) or reduction (that is, $dcc^{lox/+}DAT^{cre}$; conditional *dcc* heterozygous) of *dcc* expression by individual DA neurons would affect their survival, we conducted stereological counts of DA neurons in the VTA and substantia nigra pars compacta (SNc) and found no differences in cell counts across genotypes (Figure 2e).

Both $dcc^{lox/+}$DAT^{cre} and $dcc^{lox/lox}DAT^{cre}$ genotypes survive to adulthood and do not exhibit any overt phenotypic differences from control *dcc*-floxed littermates upon broad physical inspection. We examined both $dcc^{lox/+}$DAT^{cre} and $dcc^{lox/lox}$DAT^{cre} mice in our studies in order to study the effects of inducing either a reduction or an absence of DCC expression in individual DA neurons. Subtle variations in DCC expression are of particular interest to us because they appear to be linked to individual differences in susceptibility to DA-related psychopathology.[22,26]

DCC expression by DA neurons is required for appropriate innervation to the mPFC. To assess the role of DCC function within DA neurons on the development of mesocorticolimbic DA circuitry, we first quantified the total number of DA presynaptic terminals in the mPFC and NAcc of adult conditional mice ($dcc^{lox/+}$DAT^{cre} and $dcc^{lox/lox}DAT^{cre}$) and *dcc*-floxed control littermates. We examined cingulate 1 and prelimbic subregions of the pregenual mPFC. TH-positive varicosities were used as the counting unit to obtain a measure of DA presynaptic terminal density.[27] Although norepinephrine neurons also innervate the mPFC, the TH antibody we used rarely co-labels with norepinephrine fibers in this region.[28] Stereological counts of DA varicosities within the mesocortical DA projection were performed on tracings around the dense TH-positive fiber innervation to the mPFC inner layers. We first delineated each traced region on micrographs taken with a ×5 objective to clearly distinguish this heavily innervated area from the other more superficial cortical layers.[13]

Our results show that DCC within DA neurons is required for the appropriate organization of synaptic connectivity within mPFC DA circuits. $dcc^{lox/+}$DAT^{cre} and $dcc^{lox/lox}$DAT^{cre} mice displayed a significant increase (approximately twofold) in the total number of DA varicosities in both cingulate 1 and prelimbic subregions of the mPFC (Figure 3a). Underlying this regionally selective phenotype was an increase in the span (that is, volume measurement in cubic micrometers) of the dense DA fiber innervation to the inner layers of these subregions; DA varicosity density, however, was not different between *dcc* conditional mice and *dcc*-floxed controls (Figure 3a). The volume of the DA projection to the mPFC inner layers was estimated from the

Figure 2. Conditional deletion of exon 23 of the *dcc* gene produces a loss-of-function mutation in DA neurons. Mice were engineered to carry a mutation in the *dcc* gene exclusively *within* dopamine neurons using the Cre-loxP recombination system. (**a**) The schematic illustrates how Cre-mediated recombination of the *dcc* gene will be triggered in mice from this line if they carry (1) LoxP sequences flanking exon 23 of *dcc* and (2) a Cre-recombinase insertion that is under transcriptional control by the DAT promoter. A PCR performed on genomic DNA obtained from tissue punches taken from the ventral tegmental area (VTA) using the primer pair represented in the schematic did not yield a PCR product in *dcc*-floxed (dcc$^{lox/lox}$) control littermates. In this case, the predicted size of the PCR product in the non-recombined gene is of ~5700 bp, which is too large to amplify. However, a 374 bp product was amplified from the DNA obtained from a $dcc^{lox/lox}DAT^{cre}$ mouse, confirming successful recombination of the *dcc* gene. (**b**) The recombined *dcc* gene does not produce detectable levels of mRNA. An RT–PCR performed on cDNA of VTA tissue punches of $dcc^{lox/lox}$, $dcc^{lox/+}DAT^{cre}$ *and* $dcc^{lox/lox}DAT^{cre}$ produced two bands: (1) a larger product corresponding to the wild-type allele (arrowhead), amplified from DCC-expressing cells in the VTA that are not DAT+ DA neurons and (2) a smaller product corresponding to the recombined mRNA (arrow), which was barely above detectable levels. (**c**) DCC expression in the VTA of $dcc^{lox/lox}$DAT^{cre} mice was markedly reduced in comparison with $dcc^{lox/lox}$ control mice. A cluster of DA neurons in the ventrolateral VTA continue to express DCC. This is a region of robust DAT expression. The reason why DCC expression persists in this grouping of cells is unknown. Scale bars = 250 μm. (**d**) Western analysis of DCC levels in the NAcc confirmed a marked reduction in DCC expression in *dcc* conditional mice ($dcc^{lox/+}$DAT^{cre} and $dcc^{lox/lox}DAT^{cre}$) compared with $dcc^{lox/lox}$ control littermates. Schematic, tissue punches (1 mm in diameter) were taken from the NAcc (core and shell; plates 15–20.[64] A significantly lower level of DCC expression was observed in both $dcc^{lox/+}DAT^{cre}$ (~54% reduction) *and* $dcc^{lox/lox}DAT^{cre}$ (~77% reduction) mice ($dcc^{lox/lox}$: $n = 4$; $dcc^{lox/+}DAT^{cre}$: $n = 4$; $dcc^{lox/lox}DAT^{cre}$: $n = 3$; one-way ANOVA, significant main effect of genotype: $F_{(2,8)} = 24.94$, $P = 0.0004$. Bonferroni's multiple comparison test (1) dcc-*floxed* and $dcc^{lox/+}DAT^{cre}$, $P = 0.0014$ and (2) dcc-floxed and $dcc^{lox/lox}DAT^{cre}$, $P = 0.0003$). (**e**) Loss of DCC expression within DA neurons does not affect their survival. Stereological estimates of total DA neuron number in the VTA and substantia nigra pars compacta (SNc). Sections spanning plates 53–63 were analyzed. [64] Representative micrograph of a TH-labeled coronal section through the VTA and SNc (see schematic) used in the stereological analysis. No differences were found across genotypes in the stereological counts of DA neurons in the VTA and SNc ($dcc^{lox/lox}$: $n = 6$; $dcc^{lox/+}DAT^{cre}$: $n = 7$; $dcc^{lox/lox}DAT^{cre}$: $n = 7$; two-way repeated measures ANOVA: no significant main effect of genotype, $F_{(2,17)} = 1.129$, $P = 0.3463$; no significant interaction, $F_{(2,17)}$, $P = 0.72$).

original tracings made around the TH-labeled fibers using the Cavalieri method. The changes in DA synaptic connectivity appear to be specific to certain mPFC subregions because volume estimates of TH-positive varicosities in the infralimbic subregion were similar across genotypes (data not shown), consistent with our previous findings.[13] Although this increase in DA input to the mPFC observed in *dcc* conditional mice has a graded distribution, with effects increasing in a ventral to dorsal manner (IL < PrL < Cg1), we have not observed a gradient of netrin-1 expression in the mPFC.[13] Notably, in light of evidence showing clear

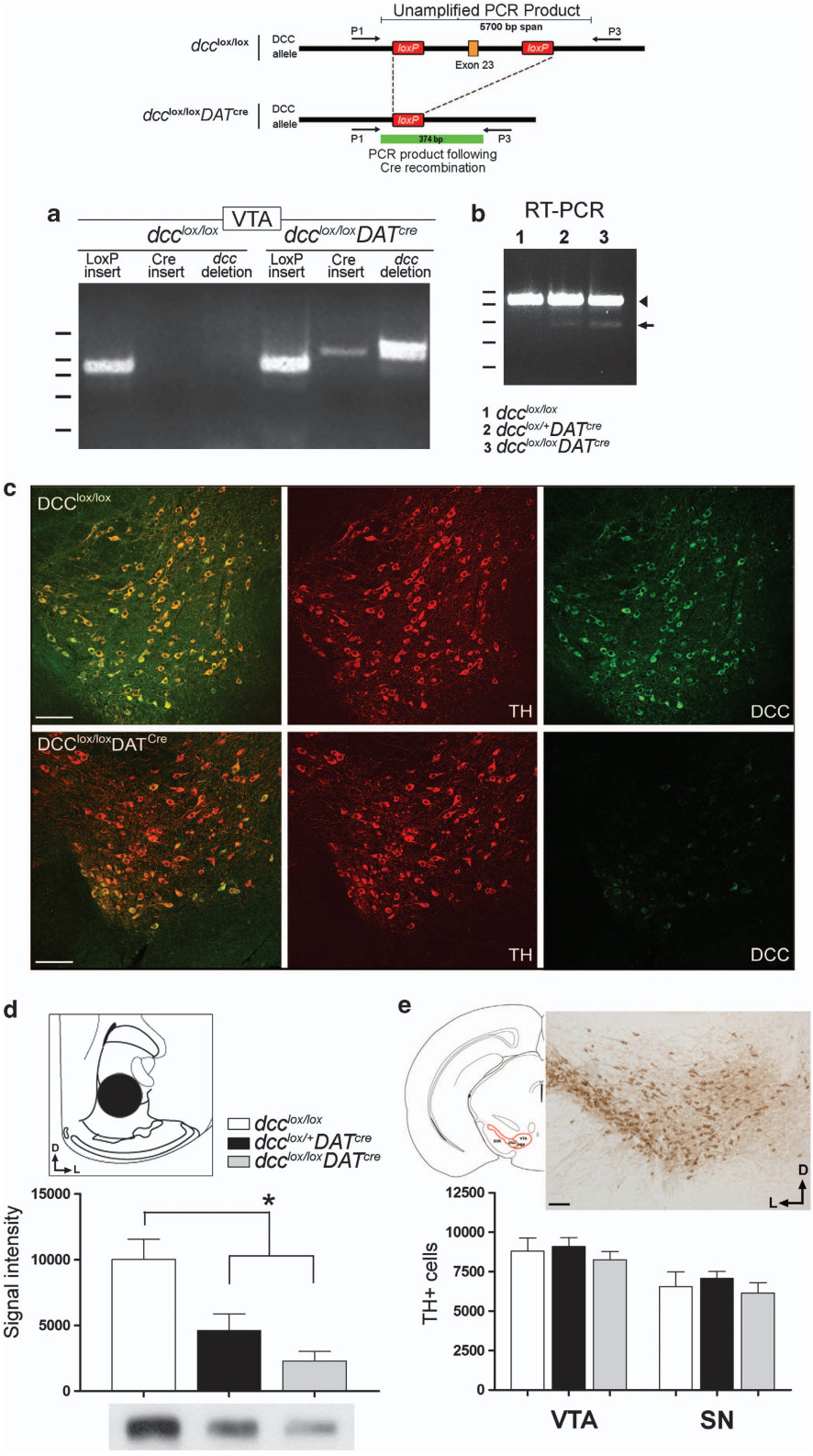

dorso-ventral distinctions in the role of the mPFC in drug-seeking behavior, *dcc* conditional mice may exhibit phenotypes in Cg1/PrL –dependent, but not IL-dependent, behaviors.[29–31]

DA synaptic changes appear to be selective to the mPFC because there are no differences in the total number of TH-positive varicosities in the NAcc across genotypes (Figure 3c). Notably, here and in our previous studies, we have found that in the NAcc all DA fibers co-label with DCC and are the exclusive source of DCC expression within this region. However, in stark contrast, a very scarce number of DA fibers express DCC in the mPFC.[13] This clear, target-dependent expression suggests that DCC has a role in the segregating DA fiber innervation between these two regions, in which the vast majority DA axons, which are DCC-positive, innervate the NAcc and only a minor subset of DA fibers, which are DCC-negative, innervate the mPFC. To test this idea, we assessed whether the enlarged span of DA innervation to the mPFC inner layers that we observed in *dcc* conditional mice coincides with an increase in the number of DCC-positive DA varicosities. We performed stereological counts of DCC/TH-positive varicosities in the mPFC of conditional *dcc* heterozygous ($dcc^{lox/+}DAT^{cre}$) and control *dcc*-floxed mice. As expected, affected DCC/TH-positive fibers in the mPFC of conditional *dcc* homozygous ($dcc^{lox/lox}DAT^{cre}$) mice were not detectable because of their complete lack of DCC expression; these fibers could not be visualized by DCC immunolabeling and therefore could not be assessed. Thus, for this analysis only mice with the $dcc^{lox/+}DAT^{cre}$ genotype could be studied. We found that indeed the density of DA varicosities expressing DCC is markedly increased in both cingulate 1 and prelimbic subregions in $dcc^{lox/+}DAT^{cre}$ mice (Figure 3b). These findings support the idea that when DCC function is disrupted, discrete regions of the mPFC receive ectopic innervation of DCC-positive DA fibers. Only sporadic DA fibers in the projection to the mPFC express DCC (~ 2%). Thus, the two- to threefold increase in DCC/TH-positive varicosities represents an increase of ~2–6% in the number of mPFC DA varicosities that express DCC. It is likely that this is an underestimate, as decreased

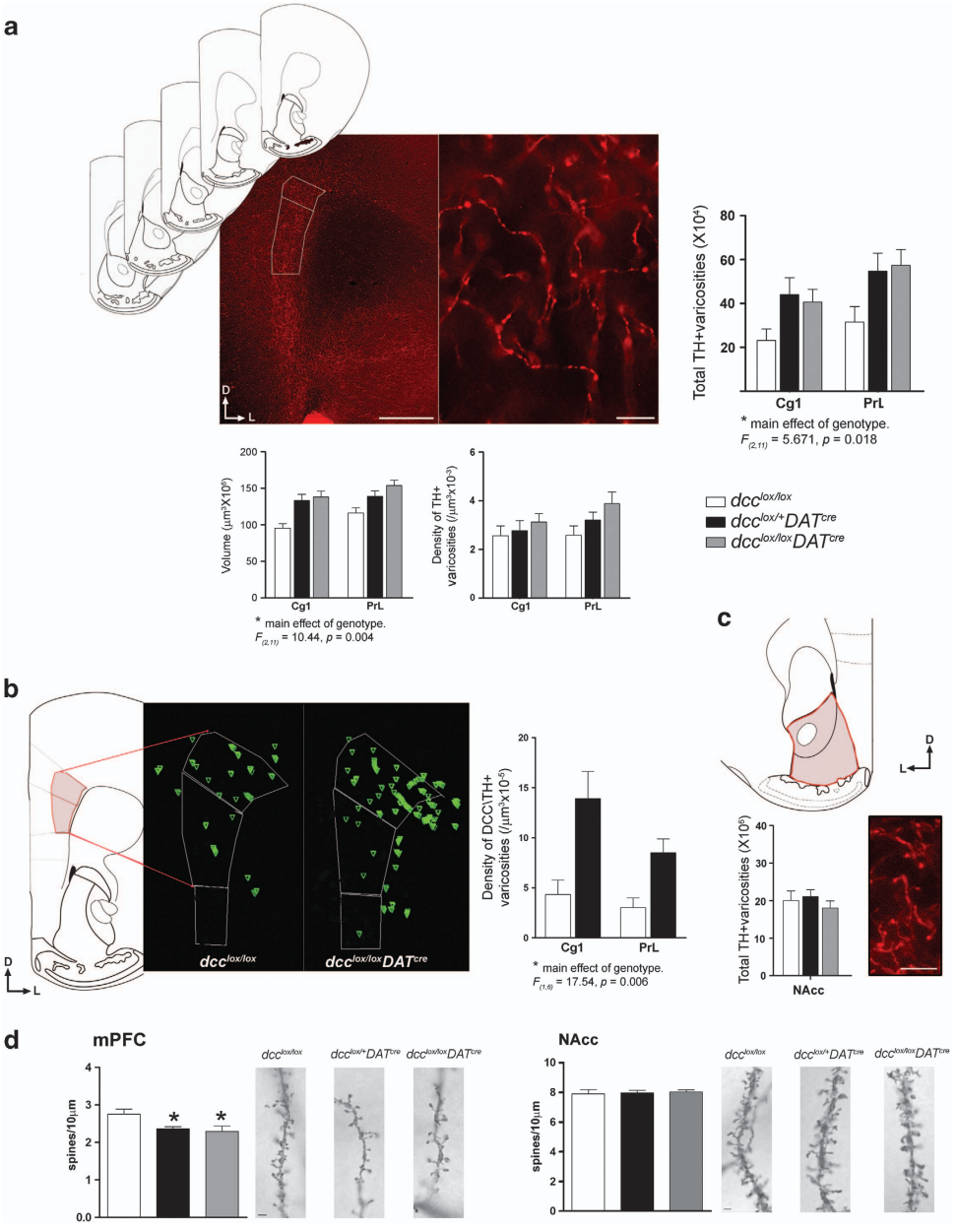

DCC expression may make it difficult to detect all ectopic DCC-positive fibers.

It is possible that these ectopic DA fibers originate from the NAcc or other non-cortical DA targets but that we are unable to detect this relative decrease in TH-positive varicosities in regions that are densely innervated with DA. Indeed, stereological counts of TH-positive varicosities indicate that the total number of varicosities in the NAcc is ~40-fold greater than in the mPFC (Figures 3a and c). Thus, the increase in the total number of TH-positive varicosities in the mPFC observed in the heterozygous and homozygous *dcc* conditional mice (Figure 3a) would correspond approximately to only 2.5% of the total number of varicosity counts obtained in the NAcc. This value is less than the s.e. of the mean number of NAcc counts (Figure 3c).

The DA projection to the mPFC continues to develop until early adulthood, and it undergoes substantial maturation during adolescence.[1–4] This gradual developmental program is unique to the mesocortical DA projection; the DA innervation to the striatum for example achieves adult density soon after birth.[4,32] Similarly, both norepinephrine and serotoninergic mPFC innervations mature early postnatally as well.[33,34] Given this protracted development, we speculated that the anatomical changes observed in the mPFC of conditional mice would only become evident in adulthood. To assess this idea, we performed stereological counts of TH-positive varicosities in the mPFC and NAcc of juvenile (PND 21) $dcc^{lox/+}DAT^{cre}$, $dcc^{lox/lox}$DAT^{cre} and *dcc*-floxed mice. Our results confirmed no differences across genotypes at this early age (see Supplementary Figure 1a, and a comparison to adult data). Furthermore, exhaustive perusal of the cingulate 1 and prelimbic mPFC subregions revealed an almost complete absence of DCC-positive DA fibers in juvenile $dcc^{lox/+}$DAT^{cre} and *dcc*-floxed mice. Together, these experiments confirm that the increased span of DA innervation to the mPFC that is observed in adult *dcc* conditional mice has not yet emerged in juvenile PND 21 mice, and suggest that *dcc* expression by DA neurons plays a role in the development of their mPFC projection during adolescence.

DCC-directed DA innervation to the mPFC determines pyramidal neuron dendritic spine density. We next asked whether the effects of DCC within DA neurons on mesocortical DA innervation would also dictate the structure of postsynaptic neurons and the resulting architecture of local mPFC circuitry. In our previous studies we showed that Layer V pyramidal neurons of adult, but not juvenile, *dcc* haploinsufficient mice have reduced dendritic spine densities,[13,17] which we show here are associated with reduced neuronal excitability (Figures 1a and c). Layer V pyramidal neurons express low levels of DCC.[13] Therefore, it is unclear whether the changes observed in these neurons in *dcc* haploinsufficient mice are cell autonomous or a consequence of the altered DA innervation. Notably, layer V receives the densest DA innervation in the mPFC.[35] In the present study, we could dissociate these two events using conditional mice.

Both $dcc^{lox/+}$DAT^{cre} and $dcc^{lox/lox}$DAT^{cre} mice showed a significant reduction in dendritic spine density of layer V pyramidal neurons compared with *dcc*-floxed control littermates (Figure 3d). These alterations were indistinguishable between *dcc* heterozygous and homozygous conditional mice. We did not observe any alterations in dendritic spine density in NAcc medium spiny neurons across genotypes (Figure 3d). Thus, our results establish that when DCC function is compromised, the neuroanatomical changes observed in mPFC pyramidal neurons are a *consequence* of altered DA innervation. These findings show that during normal postnatal development DCC-directed DA innervation can determine the organization of local mPFC DA circuitry. These effects of *dcc* may interact with those of proteins that have recently been

Figure 3. Conditional *dcc* loss-of-function *within* DA neurons, exclusively, increases DCC-expressing dopamine synaptic sites in the mPFC and postsynaptic structural changes in mPFC layer V pyramidal neurons. (**a**) Coronal sections through the pregenual mPFC (plates 14–18;[64]) were immunolabeled with TH for stereological analysis of DA varicosity innervation to the cortical inner layers. Left panel, micrograph illustrating how contours were drawn around the TH-positive fiber innervation to the mPFC inner layers within each subregion of interest (Cg1, PrL; see white tracing). Scale bar = 500 μm. Right panel, representative micrograph of TH-positive immunoreactivity in the mPFC inner layers that was used for stereological counting (taken with a ×100 objective). TH-positive varicosities were defined as dilated elements associated with axonal processes. Scale bar = 10 μm. Stereological estimates of total TH-positive varicosity number was estimated using a stereological fractionator sampling design, with the optical fractionator probe of the Stereo Investigator software. Conditional *dcc* mice exhibited an increase in the total number of TH-positive varicosities innervating the inner layers of the mPFC ($dcc^{lox/lox}$: $n = 5$; $dcc^{lox/+}DAT^{cre}$: $n = 4$; $dcc^{lox/lox}DAT^{cre}$: $n = 5$; two-way repeated measures ANOVA, main effect of genotype: $F_{(2,11)} = 5.362$, $P = 0.0293$; main effect of mPFC subregion (repeated measure): $F_{(1,11)} = 21.34$, $P = 0.0013$; no significant interaction: $F_{(2,11)} = 0.898$, $P = 0.4410$). Underlying this increase was a larger volume of dense TH-positive innervation of the mPFC inner layers (two-way repeated measures ANOVA, main effect of genotype: $F_{(2,11)} = 5.046$, $P = 0.028$; main effect of mPFC subregion (repeated measure): $F_{(1,11)} = 18.03$, $P = 0.0014$; no significant interaction: $F_{(2,11)} = 1.653$, $P = 0.236$). There were no differences in the density of TH-positive innervation (two-way repeated measures ANOVA, no main effect of genotype: $F_{(2,11)} = 1.583$, $P = 0.249$; main effect of mPFC subregion (repeated measure): $F_{(1,11)} = 9.816$, $P = 0.0095$; no significant interaction: $F_{(2,11)} = 3.062$, $P = 0.0877$). Note: while our two-way ANOVAs revealed main effects of genotype in (1) the total TH-positive varicosity number and (2) volume of TH-positive innervation, the presence of a significant interaction between genotype and mPFC subregion was not detected. Therefore, *post hoc* analyses were not required. (**b**) Conditional *dcc* mice exhibited an increase in DA innervation to the mPFC inner layers by DA varicosities that were double-labeled with DCC. Schematics generated by Neurolucida explorer (Microbrightfield) illustrating the distribution of DCC/TH-positive (green triangles) varicosity counts made within the dense TH-positive projection in one brain section (see red tracing in schematic) in a $dcc^{lox/lox}$ versus $dcc^{lox/+}DAT^{cre}$ mouse. The counts for each brain were performed across five coronal sections through the pregenual mPFC. The mean density of DCC/TH-positive varicosities was increased two- to threefold in the Cg1 and PrL in comparison with wild-type littermates ($dcc^{lox/lox}$: $n = 4$; $dcc^{lox/+}DAT^{cre}$: $n = 4$; two-way repeated measures ANOVA, main effect of genotype: $F_{(1,6)} = 17.54$, $P = 0.006$; main effect of mPFC cortex subregion (repeated measure): $F_{(1,6)} = 3.97$, $P = 0.094$; no significant interaction: $F_{(1,6)} = 1.471$, $P = 0.271$). Note: while our two-way ANOVA revealed a main effect of genotype in the density of DCC/TH-positive varicosities in the mPFC, the presence of a significant interaction between genotype and mPFC cortex subregion was not detected. *Post hoc* analyses were therefore not required. (**c**) There was no difference between genotypes in the total number of TH-positive varicosities in the NAcc ($dcc^{lox/lox}$: $n = 4$; $dcc^{lox/+}DAT^{cre}$: $n = 4$; $dcc^{lox/lox}DAT^{cre}$: $n = 4$; one-way ANOVA, no main effect of genotype, $F_{(2,9)} = 0.556$, $P = 0.5918$). (**d**) Conditional *dcc* loss-of-function *within* DA neurons, exclusively, produces postsynaptic structural changes in mPFC Layer V pyramidal neurons. The density of Layer V pyramidal neuron basilar dendritic spines is significantly lower in $dcc^{lox/+}$DAT^{cre} and $dcc^{lox/lox}$DAT^{cre} mice relative to control *dcc*-floxed littermates ($dcc^{lox/lox}$: $n = 10$; $dcc^{lox/+}DAT^{cre}$: $n = 10$; $dcc^{lox/lox}DAT^{cre}$: $n = 8$; one-way ANOVA, significant main effect of genotype: $F_{(2,25)} = 4.724$, $P = 0.0182$; Tukey's multiple comparison test: (1) $dcc^{lox/lox}$ and $dcc^{lox/+}DAT^{cre}$, $P = 0.05$), (2) dcc$^{lox/lox}$ and $dcc^{lox/lox}DAT^{cre}$, $P = 0.0276$)). Representative micrographs of Golg–Cox-labeled layer V pyramidal neuron basilar dendritic spines in $dcc^{lox/lox}$, $dcc^{lox/+}DAT^{cre}$, and $dcc^{lox/lox}$DAT^{cre} mice. Scale bar = 5 μm. Structural changes were not observed in NAcc medium spiny neurons ($dcc^{lox/lox}$: $n = 7$; $dcc^{lox/+}DAT^{cre}$: $n = 8$; $dcc^{lox/lox}DAT^{cre}$: $n = 7$; one-way ANOVA, no significant main effect of genotype: $F_{(2,19)} = 0.086$, $P = 0.915$). Representative micrographs of Golgi–Cox-labeled medium spiny neurons in $dcc^{lox/lox}$, $dcc^{lox/+}DAT^{cre}$, and $dcc^{lox/lox}$DAT^{cre} mice. Scale bar = 5 μm.

reported to influence the structure and function of developing pyramidal neurons in the postnatal PFC.[36] These results suggest that the functional phenotypes observed in the mPFC of *dcc* haploinsufficient will also be recapitulated in *dcc* conditional mice. We are currently examining the electrophysiological properties of layer V pyramidal neurons, and mPFC-dependent cognitive processing, in adolescent and adult $dcc^{lox/+}DAT^{cre}$ and $dcc^{lox/lox}DAT^{cre}$ mice.

Behavioral phenotypes of dcc conditional mice. We then tested behaviors that require the coordinated function of DA in the NAcc and mPFC. Specifically, we assessed behavioral indices of DA function that emerge in response to the stimulant drug amphetamine. Adult $dcc^{lox/+}DAT^{cre}$ and $dcc^{lox/lox}DAT^{cre}$ mice did not exhibit different locomotor activity from control *dcc*-floxed littermates either at baseline or following a single injection of saline (Figure 4a). However, when these mice were given an injection of 2.5 mg kg^{-1} of d-amphetamine sulphate, both $dcc^{lox/+}DAT^{cre}$ and $dcc^{lox/lox}DAT^{cre}$ showed blunted locomotor responses relative to *dcc*-floxed littermate controls. Drug-induced locomotion between $dcc^{lox/+}DAT^{cre}$ and $dcc^{lox/lox}DAT^{cre}$ mice was not statistically different. There were no differences in stereotype counts across genotypes, ruling out the possibility that the measures of locomotion were affected by genotypic differences in drug-induced stereotype (data not shown). Remarkably, reduced sensitivity to amphetamine in conditional mice only emerged in

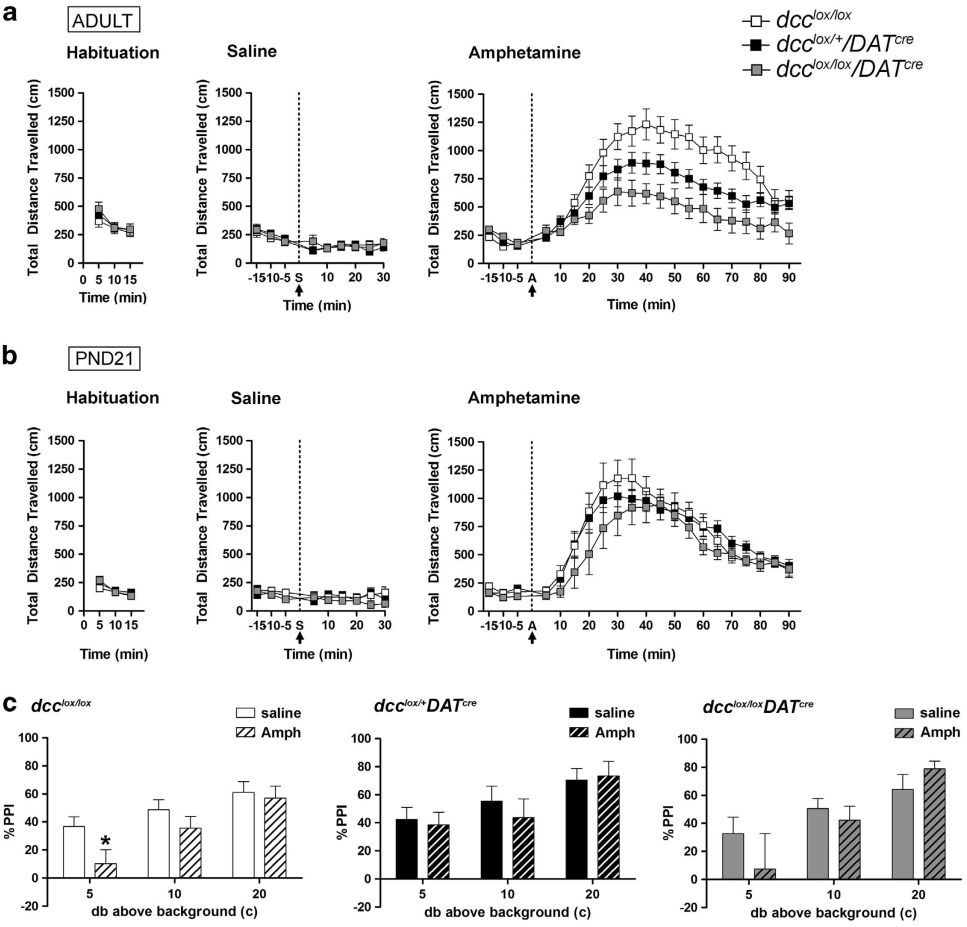

Figure 4. *dcc* conditional mice exhibit blunted behavioral responses to amphetamine only in adulthood. (**a**) There were no differences across genotypes in locomotor activity, either at baseline ($dcc^{lox/lox}$: $n=11$; $dcc^{lox/+}DAT^{cre}$: $n=12$; $dcc^{lox/lox}DAT^{cre}$: $n=7$; two-way repeated measures ANOVA, no significant main effect of genotype: $F_{(2,26)}=0.1123$, $P=0.894$; no significant interaction: $F_{(4,52)}=0.996$, $P=0.418$) or following a single injection of saline (two-way repeated measures ANOVA, no significant main effect of genotype: $F_{(2,26)}=0.481$, $P=0.623$; no significant interaction: $F_{(16,208)}=0.786$, $P=0.70$). However, *dcc* conditional mice ($dcc^{lox/+}DAT^{cre}$ and $dcc^{lox/lox}DAT^{cre}$) exhibited reduced locomotor activity following an acute injection of amphetamine relative to *dcc*-floxed control littermates (two-way repeated measures ANOVA, significant main effect of genotype: $F_{(2,\ 27)}=6.747$, $P=0.0042$; significant interaction: $F_{(40,\ 540)}=5.104$, $P<0.0001$). (**b**) Remarkably, juvenile *dcc* conditional mice did not exhibit blunted responses to amphetamine. No significant differences were observed across genotypes in locomotor activity at baseline (two-way repeated measures ANOVA, no significant main effect of genotype: $F_{(2,\ 42)}=0.528$, $P=0.597$; no significant interaction: $F_{(4,42)}=1.085$, $P=0.376$), following a single injection of saline (two-way repeated measures, no significant main effect of genotype: $F_{(2,168)}=0.912$, $P=0.417$; no significant interaction: $F_{(16,168)}=0.979$, $P=0.481$), or following a single acute injection of amphetamine (two-way repeated measures ANOVA, no significant main effect of genotype: $F_{(2,\ 420)}=1.072$, $P=0.36$; no significant interaction: $F_{(40,\ 420)}=0.894$, $P=0.657$). (**c**) *dcc* conditional mice exhibited resilience to amphetamine-induced deficits in sensorimotor gating. *dcc*-floxed littermate controls exhibited an impairment in pre-pulse inhibition at lower pre-pulses following an amphetamine (2.8 mg kg^{-1}) challenge ($dcc^{lox/lox}{}_{amph}$: $n=10$, $dcc^{lox/lox}{}_{saline}$; $n=9$ two-way repeated measures ANOVA, main effect of treatment: $F_{(1,17)}=1.68$, $P=0.212$; significant interaction: $F_{(17,\ 85)}=3.01$, $P=0.0149$. A *post hoc* ANOVA test for simple effects indicated a significant effect of treatment at the 5 db prepulse ($F_{(1,102)}=4.48$, $P=0.0443$). However, amphetamine did not produce a deficit in prepulse inhibition in $dcc^{lox/+}DAT^{cre}$ *or* $dcc^{lox/lox}DAT^{cre}$ mice ($dcc^{lox/+}DAT^{cre}{}_{amph}$: $n=8$, $dcc^{lox/+}DAT^{cre}{}_{saline}$: $n=9$; two-way repeated measures ANOVA, no main effect of treatment: $F_{(1,15)}=0.0$, $P=0.987$, no significant interaction: $F_{(5,75)}=.78$, $P=0.569$; $dcc^{lox/lox}DAT^{cre}{}_{amph}$: $n=8$, $dcc^{lox/lox}DAT^{cre}{}_{saline}$: $n=8$; two-way repeated measures ANOVA, no main effect of treatment: $F_{(1,14)}=0.31$, $P=0.588$, no significant interaction: $F_{(5,70)}=2.03$, $P=0.085$).

adulthood (Figure 4b). These data recapitulate our previous findings showing blunted locomotor responses to stimulant drugs of abuse in adult, but not in postnatal day 21 ± 1 or postnatal day 35 ± 2, *dcc* haploinsufficient mice.[17,22,37] Amphetamine-induced locomotion is dependent on DA release in the NAcc, but this can be modulated by DA transmission in the mPFC.[38–40] We have proposed that increased DA innervation and enhanced DA concentrations in the mPFC of adult mice that develop with compromised *dcc* function underlies the blunted locomotor phenotype in these mice in adulthood.[17,22,37] We recently conducted a study that supports this idea; preliminary data indicate that removal of mPFC DA transmission in adult *dcc*

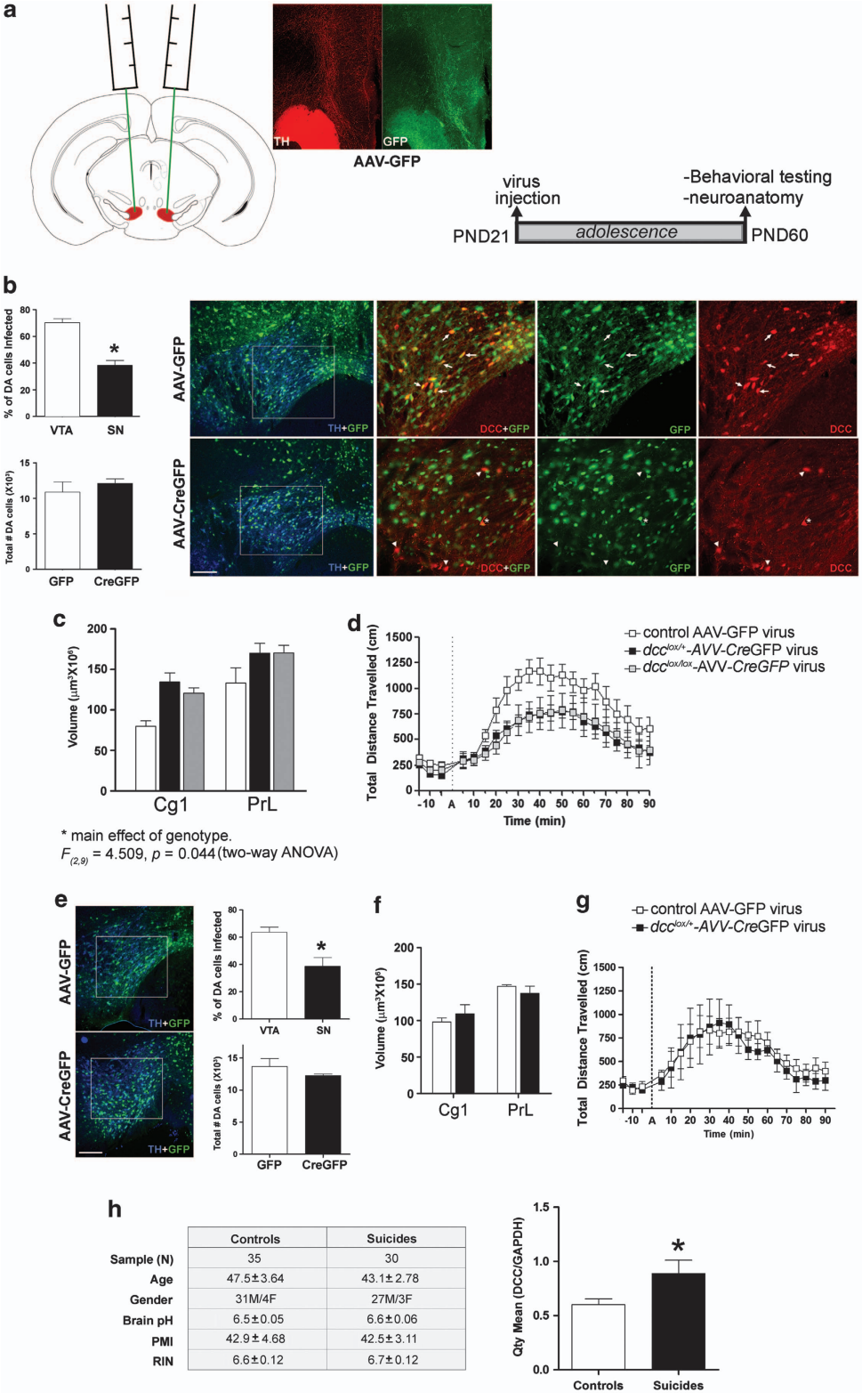

	Controls	Suicides
Sample (N)	35	30
Age	47.5±3.64	43.1±2.78
Gender	31M/4F	27M/3F
Brain pH	6.5±0.05	6.6±0.06
PMI	42.9±4.68	42.5±3.11
RIN	6.6±0.12	6.7±0.12

haploinsufficient mice reverses their blunted amphetamine-induced locomotion (MP and CF, unpublished observations).

We then assessed differences in sensorimotor-gating function across genotypes using the prepulse inhibition test. Prepulse inhibition measures the ability of a mild stimulus (prepulse) to suppress the startle response elicited by a subsequent stronger stimulus and depends on mesocorticolimbic DA function.[41] We found no differences across genotypes in baseline prepulse inhibition (data not shown). However, control *dcc*-floxed mice exhibited impaired prepulse inhibition following a single injection of 2.8 mg kg^{-1} of amphetamine, consistent with previous reports.[17] In contrast, *dcc*$^{lox/+}$DAT^{cre} and *dcc*$^{lox/lox}$DAT^{cre} mice were resilient to amphetamine-induced deficits in prepulse inhibition (Figure 4c). Notably, in this particular test, the *dcc*$^{lox/lox}$DAT^{cre} group consistently exhibited a mean response that had a high degree of variance. Closer inspection indicated that the data set did not have a bimodal distribution. Our findings confirm that behavioral responses to stimulant drugs of abuse that engage mesocorticolimbic DA function are attenuated in animals that develop with compromised DCC function within DA neurons only. Altered DA-dependent responses to stimulant drugs of abuse have been reported by subjects with psychopathologies associated with mPFC dysfunction, including schizophrenia, depression and drug abuse.[42–44] Our findings suggest that reduced *dcc* confers resilience to developing these abnormalities.

The organization of mPFC DA circuitry requires DCC during adolescence. Our results show that DCC within DA neurons is required for the appropriate organization of mesocortical DA connectivity during a specific developmental time window, which appears to coincide with adolescence. Here we asked whether compromising DCC function in adolescence would be sufficient to produce the same anatomical and behavioral phenotypes in adulthood that are exhibited by the *dcc* conditional mice. We defined early adolescence as postnatal day 21–32, mid-adolescence as postnatal day 33–44 and late adolescence as postnatal day 45–60.[6] We used an adeno-associated virus (AAV) vector expressing Cre-recombinase fused with green fluorescence protein (GFP)[19,45] to delete exon 23 of the *dcc* gene. We employed the AAV-2 strain, which conveys selective expression in neurons with no potential for retrograde infection of afferent inputs, limiting the deletion to local neuronal cell bodies.[46] AAV-CreGFP or AAV-expressing GFP alone as a control (AAV-GFP) were microinjected bilaterally into the VTA of *dcc*-floxed mice. In the VTA, dopamine neuron infection with this AAV peaks at ~2–3 weeks after injection.[19] Thus, we performed the viral microinfusions at postnatal day 21 to reach maximal infection rates during adolescence**.** To study the effects of both *dcc* reduction and *dcc* loss in individual neurons, we injected both heterozygous *dcc*-floxed (*dcc*$^{lox/+}$) and homozygous *dcc*-floxed (*dcc*$^{lox/lox}$) mice that were allowed to develop normally until the onset of early

Figure 5. Viral-mediated recombination during adolescence produces the same anatomical and behavioral adult phenotypes exhibited by *dcc* conditional mice. (**a**) Schematics, AAV-CreGFP or control AAV-GFP viruses were microinjected bilaterally into the VTA of juvenile (PND 21) heterozygous and homozygous *dcc*-floxed mice (*dcc*$^{lox/+}$ and *dcc*$^{lox/lox}$). In adulthood (PND 60-15), (1) amphetamine-induced locomotor activity and (2) the extent of DA innervation to the mPFC were measured. Micrographs show the distribution of the control AAV-GFP virus (green) in the TH-positive fibers (red) in the NAcc and mPFC, providing validation of successful infection of mesocorticolimbic projecting VTA DA neurons. Scale bar = 500 μm. (**b**) Stereological analysis of VTA and SNc DA neurons showed that, as expected, more DA neurons were infected with the AAV-CreGFP virus in the targeted VTA than in the SNc (VTA: $n = 11$ and SNc: $n = 11$, $t_{(20)} = 6.775$, $P < 0.0001$). Consistent with previous reports, an average of ~70% of DA neurons were infected.[19] Stereological estimates of total DA cell number were the same across virus treatment groups and were comparable to the numbers reported in the wild-type mouse brain (AAV-GFP: $n = 4$ and AAV-CreGFP: $n = 11$; $t_{(13)} = 0.902$, $P = 0.383$). This indicates that neither the viral infection procedure nor the loss of DCC expression affected DA neuron survival. Brain sections through the VTA of adult *dcc*$^{lox/lox}$ mice injected with the AAV-CreGFP or control AAV-GFP viruses in adolescence were triple immunolabeled with TH (blue), GFP (green) and DCC (red). A robust decrease in DCC immunoreactivity was observed in TH-positive DA neurons infected with the AAV-CreGFP virus but not with the control AAV-GFP. Scale bars = 500 μm. (**c**) Reduction or complete removal of DCC from individual VTA neurons from early adolescence onward is sufficient to reproduce the adult phenotypes observed in *dcc* conditional mice. *dcc*$^{lox/+}$ *and dcc*$^{lox/lox}$ mice that received injections of AAV-CreGFP in early adolescence had an enlarged volume of TH-positive dense fiber innervation to the cortical inner layers in adulthood relative to *dcc*-floxed mice that received injections of AAV-GFP (control AAV-GFP virus group: $n = 3$, dcc$^{lox/+}$-CreGPF virus: $n = 5$, *dcc*$^{lox/lox}$-CreGPF virus: $n = 4$; Two-way repeated measures ANOVA, main effect of genotype-virus group: $F_{(2,9)} = 5.498$, $P = 0.0275$; main effect of mPFC cortex subregion (repeated measure): $F_{(1,9)} = 47.53$, $P < 0.0001$; no significant interaction: $F_{(2,9)} = 0.686$, $P = 0.528$). Note: while our two-way ANOVA revealed a main effect of genotype-virus group in the volume of TH-positive innervation to the mPFC inner layers, the presence of a significant interaction between genotype-virus and mPFC cortex subregion was not detected. *Post hoc* analyses were therefore not required. (**d**) Compromising DCC expression in VTA neurons from early adolescence also reproduced the blunted behavioral responses to amphetamine observed in the adult *dcc* conditional mice. Both dcc$^{lox/+}$-CreGFP and *dcc*$^{lox/lox}$-CreGPF mice exhibited reduced locomotor activity in the first hour after an amphetamine challenged (2.5 mg kg^{-1}), in comparison with *dcc*-floxed mice injected with the control virus (control AAV-GFP virus group: $n = 6$, dcc$^{lox/+}$-CreGPF: $n = 7$, *dcc*$^{lox/lox}$-CreGPF: $n = 6$; two-way repeated measures ANOVA, significant main effect of genotype: $F_{(2,\ 16)} = 4.089$, $P = 0.0368$; significant interaction: $F_{(28,\ 224)} = 1.952$, $P = 0.0042$). (**e**–**g**) To assess the effects of reducing *dcc* in adult *dcc*-floxed mice that developed normally, virus microinfusions were done at PND 60. Behavioral and stereological experiments were performed 4–5 weeks after surgery. (**e**) Representative micrographs of sections through the VTA of *dcc*$^{lox/+}$ mice injected with the AAV-CreGFP or control AAV-GFP viruses in adulthood. Sections double-immunolabeled with TH (blue) and GFP (green) show TH-positive DA neurons in the VTA infected with virus. Scale bars = 500 μm. Stereological analysis of VTA and SNc DA neurons infected with the AAV-CreGFP virus shows a greater percentage of DA neurons infected in the targeted VTA than in the SNc (VTA: $n = 3$ and SNc: $n = 3$, $t_{(4)} = 3.343$, $P < 0.029$). Estimates of total DA neuron number in both virus treatment groups are consistent with previous reports on DA cell number in the normal adult mouse brain (AAV-GFP: $n = 3$ and AAV-CreGFP: $n = 3$; $t_{(4)} = 1.141$, $P = 0.317$). (**f**) *dcc*$^{lox/+}$ mice that received injections of AAV-CreGFP in adulthood did not exhibit an increased volume of DA fiber innervation to the cortical inner layers in comparison with mice that received the control AAV-GFP virus (control AAV-GFP virus: $n = 3$, dcc$^{lox/+}$-CreGPF virus: $n = 3$; two-way repeated measures ANOVA, no main effect of genotype: $F_{(1,4)} = 0.004$, $P = 0.954$; main effect of region (repeated measure): $F_{(1,4)} = 99.73$, $P = 0.0006$; no significant interaction: $F_{(1,4)} = 7.418$, $P = 0.053$). (**g**) In heterozygous *dcc*-floxed mice, compromising DCC expression in VTA neurons in adulthood did not lead to blunted behavioral responses to amphetamine compared with mice that received the control AAV-GFP virus. dcc$^{lox/+}$-CreGFP mice exhibited a similar level of locomotor activity as control dcc$^{lox/+}$-GFP mice in the first hour after a 2.5 mg kg^{-1} amphetamine challenge (control AAV-GFP virus group: $n = 6$, dcc$^{lox/+}$-CreGFP: $n = 7$; two-way repeated measures ANOVA, no main effect of genotype: $F_{(1,\ 6)} = 0.070$, $P = 0.7996$; no interaction: $F_{(20,\ 120)} = 0.263$, $P = 0.999$). (**h**) Brain expression of *DCC* is elevated in depressed suicide completers. *DCC* mRNA levels in prefrontal cortex tissue (BA44) obtained from the Quebec Suicide Brain Bank were assessed using qRT–PCR. Brains were matched for individual age and gender, brain pH and postmortem interval (PMI). Mean RNA integrity numbers (RIN) were between 6 and 7. Remarkably, *DCC* levels were 48% higher in suicide completers in comparison with control subjects ($t_{(63)} = 2.287$, $^*P < 0.026$). Group mean ± s.e.m. of AQ values from qRT–PCR were normalized to GAPDH.

adolescence (postnatal day 21). When mice reached adulthood, we measured *(a)* their locomotor activity and *(b)* the number DA varicosities in the mPFC (Figures 5a and d).

Stereological analysis of adult homozygous *dcc*-floxed brains confirmed that the AAV-CreGFP virus microinjections predominantly infected VTA DA neurons, in comparison with the number of DA neurons infected in the SNc (Figure 5b). Consistent with previous reports, ~70% of VTA DA neurons were infected with AAV-CreGFP virus[19]; Figure 5b). A similar level of infection was observed with the control AAV-GFP virus (data not shown). Infection with the AAV-GFP control virus or with AAV-CreGFP (along with the accompanying loss of DCC expression) did not compromise DA neuron survival. Stereological estimates of DA cell number were consistent with previous reports in the normal mouse brain and were not different across genotypes (Figure 5b). Immunohistochemical labeling of brain sections through the VTA from homozygous *dcc*-floxed mice injected with AAV-CreGFP virus showed a clear absence of DCC immunoreactivity in TH-positive neurons expressing CreGFP (Figure 5b). This confirmed that TH-positive neurons infected with AAV-CreGFP undergo recombination of the *dcc* gene and loss of DCC protein expression. Injection placements were confirmed at this time.

Reduction or complete removal of DCC from individual VTA neurons from early adolescence onward is sufficient to reproduce the selective increase in DA innervation to the mPFC observed in adult *dcc* conditional mice. Cavalieri estimates revealed an enlarged span of DA innervation to the inner layers of the mPFC in both AAV-CreGFP-infected heterozygous and homozygous *dcc*-floxed adult mice (Figure 5c). Notably, this effect was observed in the cingulate 1 and prelimbic subregions. Furthermore, reduction or complete removal of DCC from individual VTA neurons from adolescence also reproduced the blunted behavioral responses to amphetamine observed in the adult *dcc* conditional mice. Both AAV-CreGFP-infected heterozygous and homozygous *dcc*-floxed mice exhibited reduced locomotor activity when challenged with an injection of 2.5 mg kg^{-1} of amphetamine in adulthood, in comparison with mice injected with the control virus (Figure 5d). All groups showed similar locomotor activity at baseline and following a systemic injection of saline (data not shown). Significantly, the extent of the increase in DA innervation to the mPFC and the level of reduction in sensitivity to the behavioral effects of amphetamine were identical between heterozygous and homozygous *dcc*-floxed mice injected with AAV-CreGFP.

Our results indicate that reducing *dcc* expression beginning in early adolescence reproduces the adult phenotypes observed in the *dcc* conditional mice. These findings suggest a specific role for *dcc* in the development of mesocortical DA projections during adolescence. However, in this study we could not rule out the possibility that a reduction in *dcc* in adulthood, specifically, underlies these phenotypes. We therefore induced viral Cre-mediated recombination of *dcc* in adult heterozygous *dcc*-floxed mice (PND 60). A 1-month period following virus infusion elapsed before behavioral testing and neuroanatomical experiments. Stereological analysis confirmed that the AAV-CreGFP and AAV-GFP virus microinjections infected the majority of DA neurons within the targeted VTA and did not affect DA cell survival (Figure 5e). Heterozygous *dcc*-floxed mice injected with AAV-CreGFP in adulthood did not display altered locomotor responses to amphetamine (Figure 5g). Furthermore, *dcc*-floxed mice infected with AAV-CreGFP did not exhibit changes in DA innervation to the mPFC (Figure 5f). These results confirm that the adult phenotypes induced in *dcc*-floxed mice receiving viral Cre in early adolescence result from compromised DCC function during adolescent development, specifically.

Taken together, these studies reveal the remarkable finding that *dcc* function within DA neurons is required for the development of their mPFC connectivity during adolescence: (1) *dcc* conditional mice do not exhibit any DA-related phenotypes as juveniles, (2) viral studies confirm that compromising *dcc* function from early adolescence reproduces the phenotypes we observed in adult *dcc* conditional mice and (3) reducing *dcc* expression in adult *dcc*-floxed mice that were allowed to develop normally does not induce these phenotypes. To date, the study of cellular and molecular events underlying the development of DA neurons has been focused on the embryonic and early postnatal periods. However, adolescence is becoming recognized as a crucial stage in the fine-tuning of DA circuitry. Here we identify the first gene involved exclusively in the specific period of late postnatal mesocortical DA development. The implications of our present study are far-reaching. In humans, the risk of developing psychiatric disorders increases markedly during adolescence.

DCC levels are increased in depressed suicide completers

Our current findings, together with our previous reports, suggest that reduced *dcc* expression confers resilience against developing neuroanatomical, neurochemical and behavioral traits associated with mental disorders involving mPFC dysfunction.[13,17,26,37,47,48] In order to further substantiate this hypothesis, we measured the level of *DCC* expression in postmortem brains of depressed human subjects that committed suicide. We chose the BA44 because it is part of the prefrontal cortex and because a number of studies, including those conducted by the authors of the present paper, identify it as a prefrontal cortex subregion in which genes that have been associated with depression are differentially expressed.[49–52] We used quantitative real-time PCR (qRT–PCR) to assess *DCC* levels in prefrontal cortex samples of subjects from the Quebec Suicide Brain Bank (Douglas Institute). Thirty suicide completers and thirty-five age-matched sudden death controls were included in the study. Controls subjects had no life history of suicidal behavior, major psychiatric illness or antidepressant treatment. All subjects within the cohort of suicide completers had not been on antidepressants in the last 3 months leading up to their death. Remarkably, *DCC* levels were ~48% *higher* in suicide completers in comparison with control subjects (Figure 5h). These data support the idea that dysregulation of *DCC* may affect mPFC DA connectivity and that its upregulation may predispose to psychiatric illness. Our recent report linking schizophrenia to an SNP in the *DCC* gene that may be implicated in the regulation of *DCC* expression is consistent with this.[26] However, we have not yet determined the functional consequences of the SNP. We are currently determining the history of suicide attempts in the schizophrenic subjects that had the SNP. Our studies in *dcc* loss-of-function transgenic mouse models led us to propose that variations in *DCC* during development may influence predisposition to mPFC-dependent disorders in humans.[22] The findings presented here lend support to this idea.

DISCUSSION

Eclipsed by the substantial dense innervation to the striatal region, mesocortical DA synaptic inputs are very sparse. However, these exceedingly few cortical DA fibers appear to be strategically organized to profoundly influence mPFC output. Indeed, our study indicates that a subtle change in the number and in the organization of mPFC DA inputs produces structural and functional changes in layer V pyramidal neurons and is associated with marked behavioral effects. Thus, maintaining the extent of DA innervation appears crucial for shaping the architecture and function of adult mPFC circuitry. Here we provide evidence that establishes *dcc* as the first DA gene involved in this maintenance.

We propose that DCC within certain populations of mesocorticolimbic DA neurons acts on target recognition rather than on early axonal pathfinding. DCC labeling within mesocorticolimbic

DA projections is segregated to axons that innervate striatal and other limbic regions.[13] The sparse DA projection to the mPFC contains only sporadic DCC-expressing axons (~2%). This is already observed in juvenile mice and continues into adulthood. The process by which cortical and limbic DA connectivity unfolds is not well understood. However, it is known that mPFC DA neurons extend in the medial forebrain bundle along with DA axons destined to innervate limbic regions and in fact reach their cortical targets via the striatum.[1] It is possible, therefore, that DCC-negative DA axons are the only fibers to reach the cortex because DCC-expressing DA fibers undergo target recognition events earlier along their path. Impaired DCC signaling within these DA fibers may increase the likelihood of target recognition errors and result in ectopic innervation of more anterior targets by these affected DA fibers. Indeed, when DCC function within DA neurons is compromised, we observe a marked increase (approximately two- to threefold) in the number of DA fibers expressing DCC in the mPFC. A role for DCC in target recognition and axon differentiation has been described in other systems.[53–55] Certainly, the fact that *dcc* conditional heterozygous and homozygous mice do not have an altered number of DA varicosities in the NAcc and dorsal striatum supports the idea that DCC is not required for early DA axon pathfinding to this region**.** It is important to note that a complete understanding of the spatiotemporal development of the DA projection to the mPFC is lacking. In light of our current knowledge and the data that we have gathered, the proposed hypothesis is the most parsimonious. In support of our current hypothesis, a recent study indicates that new afferent fibers from the mPFC and NAcc continue to innervate the VTA between adolescence and adulthood.[56]

The functional significance of the presence of sporadic DCC-expressing mesocortical DA neurons in the normal animal is very intriguing. The fact that only a small increase in these fibers can bring about changes in the organization of mPFC DA circuitry, with marked functional consequences, suggests that these fibers serve a crucial function and that their number and connectivity is tightly regulated. The fact that a homozygous loss-of-function mutation of *dcc* does not produce a more marked phenotype than a heterozygous mutation supports this notion.

The organization of mPFC DA circuits requires DCC signaling by mesolimbic DA neurons during adolescence. How is DCC function recruited specifically during this developmental period? In our virus studies, inactivation of *dcc* from early adolescence, but not in adulthood, recapitulated the anatomical and behavioral phenotypes observed in the *dcc* conditional mice. By PND 21 DA fibers in the striatum and other limbic regions have reached their maximum density and begin to undergo an intense period of dynamic changes in activity and connectivity.[4,6,57–59] These alterations in limbic DA neurons may promote DCC signaling by increasing its translocation to the membrane surface.[60] In addition, another family of netrin-1 receptors may be involved: the UNC5 homologues. This netrin-1 receptor family signals repulsion by forming receptor complexes with DCC.[61] As such, the ratio of DCC to UNC5-homologue receptors in a cell may determine whether it will respond to netrin-1 with attraction or repulsion. UNC5C expression by DCC-positive DA neurons emerges in early adolescence and may determine the timing of when these genes influence mPFC DA organization.[12] In fact, similar to the *dcc* haploinsufficient and conditional models, we have recently shown that adult *unc5c* haploinsufficient mice exhibit a selective increase in DA innervation to the mPFC and protection against amphetamine-induced locomotion, but only after adolescence.[62] The adolescent emergence of UNC5C in DCC-expressing DA neurons may alter DCC-mediated function.[61]

Adolescence is a vulnerable period for neurodevelopmental psychiatric disorders that involve alterations in mPFC circuitry and cognitive dysfunction.[63] Our findings in the *dcc* conditional mice suggest that reduced DCC function *within* DA neurons, specifically during adolescence, confers resilience against these disorders. Support for a role of *DCC* in influencing susceptibility to psychopathology is our finding that *DCC* expression is increased in postmortem brains of depressed human subjects who committed suicide. Our recent report of an association between schizophrenia and a genetic variation in *DCC* that may involve dysregulation of DCC expression[26] further substantiates this idea. Pharmacological and prophylactic interventions earlier in life may alter DCC function in the DA system and in turn may have an impact on disease outcome. The idea of DCC as therapeutic target during adolescence is compelling given the increasing consensus that interventions at the earliest signs of disease may be more effective.

CONFLICT OF INTEREST

The authors declare no conflict of interest.

ACKNOWLEDGMENTS

This work was funded by the Canadian Institute for Health Research (C.F. MOP-74709), the Natural Science and Engineering Research Council of Canada (C.F. Grant Number 2982226) and the Fonds de la Recherche en Santé du Québec (C.F.).

REFERENCES

1 Kalsbeek A, Voorn P, Buijs RM, Pool CW, Uylings HB. Development of the dopaminergic innervation in the prefrontal cortex of the rat. *J Comp Neurol* 1988; **269**: 58–72.
2 Benes FM, Taylor JB, Cunningham MC. Convergence and plasticity of monoaminergic systems in the medial prefrontal cortex during the postnatal period: implications for the development of psychopathology. *Cereb Cortex* 2000; **10**: 1014–1027.
3 Rosenberg DR, Lewis DA. Postnatal maturation of the dopaminergic innervation of monkey prefrontal and motor cortices: a tyrosine hydroxylase immunohistochemical analysis. *J Comp Neurol* 1995; **358**: 383–400.
4 Naneix F, Marchand AR, Di Scala G, Pape JR, Coutureau E. Parallel maturation of goal-directed behavior and dopaminergic systems during adolescence. *J Neurosci* 2012; **32**: 16223–16232.
5 O'Donnell P. Adolescent onset of cortical disinhibition in schizophrenia: insights from animal models. *Schizophr Bull* 2011; **37**: 484–492.
6 Spear LP. The adolescent brain and age-related behavioral manifestations. *Neurosci Biobehav Rev* 2000; **24**: 417–463.
7 Crone EA, Dahl RE. Understanding adolescence as a period of social-affective engagement and goal flexibility. *Nature reviews Neuroscience* 2012; **13**: 636–650.
8 Weinberger DR, Berman KF, Illowsky BP. Physiological dysfunction of dorsolateral prefrontal cortex in schizophrenia. III. A new cohort and evidence for a monoaminergic mechanism. *Arch Gen Psychiatry* 1988; **45**: 609–615.
9 Merriam EP, Thase ME, Haas GL, Keshavan MS, Sweeney JA. Prefrontal cortical dysfunction in depression determined by Wisconsin Card Sorting Test performance. *Am J Psychiatry* 1999; **156**: 780–782.
10 Woicik PA, Urban C, Alia-Klein N, Henry A, Maloney T, Telang F *et al.* A pattern of perseveration in cocaine addiction may reveal neurocognitive processes implicit in the Wisconsin Card Sorting Test. *Neuropsychologia* 2011; **49**: 1660–1669.
11 Goldstein RZ, Volkow ND. Dysfunction of the prefrontal cortex in addiction: neuroimaging findings and clinical implications. *Nat Rev Neurosci* 2011; **12**: 652–669.
12 Manitt C, Labelle-Dumais C, Eng C, Grant A, Mimee A, Stroh T *et al.* Peri-pubertal emergence of UNC-5 homologue expression by dopamine neurons in rodents. *PLoS ONE* 2010; **5**: e11463.
13 Manitt C, Mimee A, Eng C, Pokinko M, Stroh T, Cooper HM *et al.* The netrin receptor DCC is required in the pubertal organization of mesocortical dopamine circuitry. *J Neurosci* 2011; **31**: 8381–8394.
14 Grant A, Speed Z, Labelle-Dumais C, Flores C. Post-pubertal emergence of a dopamine phenotype in netrin-1 receptor-deficient mice. *Eur J Neurosci* 2009; **30**: 1318–1328.
15 Srour M, Riviere JB, Pham JM, Dube MP, Girard S, Morin S *et al.* Mutations in DCC cause congenital mirror movements. *Science* 2010; **328**: 592.
16 Depienne C, Cincotta M, Billot S, Bouteiller D, Groppa S, Brochard V *et al.* A novel DCC mutation and genetic heterogeneity in congenital mirror movements. *Neurology* 2011; **76**: 260–264.
17 Grant A, Hoops D, Labelle-Dumais C, Prevost M, Rajabi H, Kolb B *et al.* Netrin-1 receptor-deficient mice show enhanced mesocortical dopamine transmission and

blunted behavioural responses to amphetamine. *Eur J Neurosci* 2007; **26**: 3215–3228.
18 Fazeli A, Dickinson SL, Hermiston ML, Tighe RV, Steen RG, Small CG *et al.* Phenotype of mice lacking functional Deleted in colorectal cancer (Dcc) gene. *Nature* 1997; **386**: 796–804.
19 Berton O, McClung CA, Dileone RJ, Krishnan V, Renthal W, Russo SJ *et al.* Essential role of BDNF in the mesolimbic dopamine pathway in social defeat stress. *Science* 2006; **311**: 864–868.
20 Birrell JM, Brown VJ. Medial frontal cortex mediates perceptual attentional set shifting in the rat. *J Neurosci* 2000; **20**: 4320–4324.
21 Dias R, Robbins TW, Roberts AC. Primate analogue of the Wisconsin Card Sorting Test: effects of excitotoxic lesions of the prefrontal cortex in the marmoset. *Behav Neurosci* 1996; **110**: 872–886.
22 Flores C. Role of netrin-1 in the organization and function of the mesocorticolimbic dopamine system. *J Psychiatry Neurosci* 2011; **36**: 296–310.
23 Krimpenfort P, Song JY, Proost N, Zevenhoven J, Jonkers J, Berns A. Deleted in colorectal carcinoma suppresses metastasis in p53-deficient mammary tumours. *Nature* 2012; **482**: 538–541.
24 Turiault M, Parnaudeau S, Milet A, Parlato R, Rouzeau JD, Lazar M *et al.* Analysis of dopamine transporter gene expression pattern -- generation of DAT-iCre transgenic mice. *FEBS J* 2007; **274**: 3568–3577.
25 Horn KE, Glasgow SD, Gobert D, Bull SJ, Luk T, Girgis J *et al.* DCC Expression by Neurons Regulates Synaptic Plasticity in the Adult Brain. *Cell Rep* 2012; **3**: 173–185.
26 Grant A, Fathalli F, Rouleau G, Joober R, Flores C. Association between schizophrenia and genetic variation in DCC: A case-control study. *Schizophr Res* 2012; **137**: 26–31.
27 Benes FM, Vincent SL, Molloy R, Khan Y. Increased interaction of dopamine-immunoreactive varicosities with GABA neurons of rat medial prefrontal cortex occurs during the postweanling period. *Synapse* 1996; **23**: 237–245.
28 Miner LH, Schroeter S, Blakely RD, Sesack SR. Ultrastructural localization of the norepinephrine transporter in superficial and deep layers of the rat prelimbic prefrontal cortex and its spatial relationship to probable dopamine terminals. *J Comp Neurol* 2003; **466**: 478–494.
29 Kalivas PW, Volkow ND. The neural basis of addiction: a pathology of motivation and choice. *Am J Psychiatry* 2005; **162**: 1403–1413.
30 Kalivas PW. Addiction as a pathology in prefrontal cortical regulation of corticostriatal habit circuitry. *Neurotox Res* 2008; **14**: 185–189.
31 Peters J, Kalivas PW, Quirk GJ. Extinction circuits for fear and addiction overlap in prefrontal cortex. *Learn Mem* 2009; **16**: 279–288.
32 Voorn P, Kalsbeek A, Jorritsma-Byham B, Groenewegen HJ. The pre- and postnatal development of the dopaminergic cell groups in the ventral mesencephalon and the dopaminergic innervation of the striatum of the rat. *Neuroscience* 1988; **25**: 857–887.
33 Levitt P, Moore RY. Development of the noradrenergic innervation of neocortex. *Brain Res* 1979; **162**: 243–259.
34 Lidov HG, Grzanna R, Molliver ME. The serotonin innervation of the cerebral cortex in the rat--an immunohistochemical analysis. *Neuroscience* 1980; **5**: 207–227.
35 Van Eden CG, Hoorneman EM, Buijs RM, Matthijssen MA, Geffard M, Uylings HB. Immunocytochemical localization of dopamine in the prefrontal cortex of the rat at the light and electron microscopical level. *Neuroscience* 1987; **22**: 849–862.
36 Iafrati J, Orejarena MJ, Lassalle O, Bouamrane L, Chavis P. Reelin, an extracellular matrix protein linked to early onset psychiatric diseases, drives postnatal development of the prefrontal cortex via GluN2B-NMDARs and the mTOR pathway. *Mol Psychiatry* advance online publication, 11 June 2013; doi:10.1038/mp.2013.66 (e-pub ahead of print).
37 Flores C, Manitt C, Rodaros D, Thompson KM, Rajabi H, Luk KC *et al.* Netrin receptor deficient mice exhibit functional reorganization of dopaminergic systems and do not sensitize to amphetamine. *Mol Psychiatry* 2005; **10**: 606–612.
38 Ventura R, Alcaro A, Cabib S, Conversi D, Mandolesi L, Puglisi-Allegra S. Dopamine in the medial prefrontal cortex controls genotype-dependent effects of amphetamine on mesoaccumbens dopamine release and locomotion. *Neuropsychopharmacology* 2004; **29**: 72–80.
39 Banks KE, Gratton A. Possible involvement of medial prefrontal cortex in amphetamine-induced sensitization of mesolimbic dopamine function. *Eur J Pharmacol* 1995; **282**: 157–167.
40 Doherty MD, Gratton A. Medial prefrontal cortical D1 receptor modulation of the meso-accumbens dopamine response to stress: an electrochemical study in freely-behaving rats. *Brain Res* 1996; **715**: 86–97.
41 Swerdlow NR, Mansbach RS, Geyer MA, Pulvirenti L, Koob GF, Braff DL. Amphetamine disruption of prepulse inhibition of acoustic startle is reversed by depletion of mesolimbic dopamine. *Psychopharmacology (Berl)* 1990; **100**: 413–416.
42 Laruelle M, Abi-Dargham A, van Dyck CH, Gil R, D'Souza CD, Erdos J *et al.* Single photon emission computerized tomography imaging of amphetamine-induced dopamine release in drug-free schizophrenic subjects. *Proc Natl Acad Sci USA* 1996; **93**: 9235–9240.
43 Tremblay LK, Naranjo CA, Cardenas L, Herrmann N, Busto UE. Probing brain reward system function in major depressive disorder: altered response to dextroamphetamine. *Arch Gen Psychiatry* 2002; **59**: 409–416.
44 Cox SM, Benkelfat C, Dagher A, Delaney JS, Durand F, McKenzie SA *et al.* Striatal dopamine responses to intranasal cocaine self-administration in humans. *Biol Psychiatry* 2009; **65**: 846–850.
45 Le Y, Miller JL, Sauer B. GFPcre fusion vectors with enhanced expression. *Anal Biochem* 1999; **270**: 334–336.
46 Bartlett JS, Samulski RJ. Fluorescent viral vectors: a new technique for the pharmacological analysis of gene therapy. *Nat Med* 1998; **4**: 635–637.
47 Yetnikoff L, Eng C, Benning S, Flores C. Netrin-1 receptor in the ventral tegmental area is required for sensitization to amphetamine. *Eur J Neurosci* 2010; **31**: 1292–1302.
48 Argento JK, Arvanitogiannis A, Flores C. Juvenile exposure to methylphenidate reduces cocaine reward and alters netrin-1 receptor expression in adulthood. *Behav Brain Res* 2012; **229**: 202–207.
49 Lopez JP, Fiori LM, Gross JA, Labonte B, Yerko V, Mechawar N *et al.* Regulatory role of miRNAs in polyamine gene expression in the prefrontal cortex of depressed suicide completers. *Int J Neuropsychopharmacol* 2013; 1–10 (e-pub ahead of print).
50 Sequeira A, Mamdani F, Ernst C, Vawter MP, Bunney WE, Lebel V *et al.* Global brain gene expression analysis links glutamatergic and GABAergic alterations to suicide and major depression. *PLoS One* 2009; **4**: e6585.
51 Klempan TA, Sequeira A, Canetti L, Lalovic A, Ernst C, ffrench-Mullen J *et al.* Altered expression of genes involved in ATP biosynthesis and GABAergic neurotransmission in the ventral prefrontal cortex of suicides with and without major depression. *Mol Psychiatry* 2009; **14**: 175–189.
52 Fiori LM, Turecki G. Broadening our horizons: gene expression profiling to help better understand the neurobiology of suicide and depression. *Neurobiol Dis* 2012; **45**: 14–22.
53 Deiner MS, Kennedy TE, Fazeli A, Serafini T, Tessier-Lavigne M, Sretavan DW. Netrin-1 and DCC mediate axon guidance locally at the optic disc: loss of function leads to optic nerve hypoplasia. *Neuron* 1997; **19**: 575–589.
54 Manitt C, Nikolakopoulou AM, Almario DR, Nguyen SA, Cohen-Cory S. Netrin participates in the development of retinotectal synaptic connectivity by modulating axon arborization and synapse formation in the developing brain. *J Neurosci* 2009; **29**: 11065–11077.
55 Colon-Ramos DA, Margeta MA, Shen K. Glia promote local synaptogenesis through UNC-6 (netrin) signaling in C. elegans. *Science* 2007; **318**: 103–106.
56 Yetnikoff L, Reichard RA, Schwartz ZM, Parsely KP, Zahm DS. Protracted maturation of forebrain afferent connections of the ventral tegmental area in the rat. *J Comp Neurol* 2013 (e-pub ahead of print).
57 McCutcheon JE, Conrad KL, Carr SB, Ford KA, McGehee DS, Marinelli M. Dopamine neurons in the ventral tegmental area fire faster in adolescent rats than in adults. *J Neurophysiol* 2012; **108**: 1620–1630.
58 Antonopoulos J, Dori I, Dinopoulos A, Chiotelli M, Parnavelas JG. Postnatal development of the dopaminergic system of the striatum in the rat. *Neuroscience* 2002; **110**: 245–256.
59 Brummelte S, Teuchert-Noodt G. Postnatal development of dopamine innervation in the amygdala and the entorhinal cortex of the gerbil (Meriones unguiculatus). *Brain Res* 2006; **1125**: 9–16.
60 Bouchard JF, Moore SW, Tritsch NX, Roux PP, Shekarabi M, Barker PA *et al.* Protein kinase A activation promotes plasma membrane insertion of DCC from an intracellular pool: A novel mechanism regulating commissural axon extension. *J Neurosci* 2004; **24**: 3040–3050.
61 Hong K, Hinck L, Nishiyama M, Poo MM, Tessier-Lavigne M, Stein E. A ligand-gated association between cytoplasmic domains of UNC5 and DCC family receptors converts netrin-induced growth cone attraction to repulsion. *Cell* 1999; **97**: 927–941.
62 Auger M, Schmidt E, Manitt C, Dal-Bo G, Pasterkamp J, Flores C. unc5c haploinsufficient phenotype: striking similarities with the dcc haploinsufficient model. *European Journal of Neuroscience* 2013; **38**: 2853–2863.
63 Anderson RB, Cooper HM, Jackson SC, Seaman C, Key B. DCC plays a role in navigation of forebrain axons across the ventral midbrain commissure in embryonic xenopus. *Dev Biol* 2000; **217**: 244–253.
64 Paxinos G, Franklin KBJ. *Paxinos and Franklin's the Mouse Brain in Stereotaxic coordinates*. 4th edn. Elsevier/Academic Press: Boston, Amsterdam, 2013.

Supplementary Information accompanies the paper on the Translational Psychiatry website (http://www.nature.com/tp)